# Skeletal Muscle Pathology in X-Linked Myotubular Myopathy: Review With Cross-Species Comparisons

*J Neuropathol Exp Neurol*
Vol. 75, No. 2, February 2016, pp. 102–110
doi: 10.1093/jnen/nlv020

OXFORD

REVIEW ARTICLE

# Skeletal Muscle Pathology in X-Linked Myotubular Myopathy: Review With Cross-Species Comparisons

Michael W. Lawlor, MD, PhD, Alan H. Beggs, PhD, Ana Buj-Bello, MD, PhD, Martin K. Childers, DO, PhD, James J. Dowling, MD, PhD, Emma S. James, PhD, Hui Meng, MD, PhD, Steven A. Moore, MD, PhD, Suyash Prasad, MBBS, MRCP, MRCPCH FFPM, Benedikt Schoser, MD, and Caroline A. Sewry, PhD

From the Division of Pediatric Pathology, Department of Pathology and Laboratory Medicine, Medical College of Wisconsin, Milwaukee, Wisconsin (MWL, HM); Division of Genetics and Genomics, The Manton Center for Orphan Disease Research, Boston Children's Hospital, Harvard Medical School, Boston, Massachusetts (AHB); Genethon, INSERM U951, Evry, France (ABB); Department of Rehabilitation Medicine, University of Washington, Seattle, Washington (MKC); Division of Neurology, Department of Pediatrics, Hospital for Sick Children, Toronto, Ontario, Canada (JJD); Audentes Therapeutics, San Francisco, California (EJ, SP); The University of Iowa, Carver College of Medicine, Department of Pathology, Iowa City, Iowa (SAM); Friedrich-Baur-Institute, Department of Neurology, Ludwig-Maximilians-University Munich, Germany (BS); Dubowitz Neuromuscular Centre, UCL Institute of Child Health/Great Ormond Street Hospital for Children, London, UK (CAS); and Wolfson Centre for Inherited Neuromuscular Diseases, RJAH Orthopaedic Hospital, Oswestry, UK (CAS)

Send correspondence to: Michael W. Lawlor, MD, PhD, 9000 W. Wisconsin Ave., TBRC Building, Room C4490, Milwaukee, WI 53226; E-mail: mlawlor@mcw.edu

This study was supported in part by funding from the National Institutes of Health grants K08 AR059750, R01 AR044345, R21 AR064503, R01 HL115001, and U54 NS053672, the Senator Paul D. Wellstone Muscular Dystrophy Cooperative Research Center, Seattle (NIH U54 AR065139), the Association Française contre les Myopathies, the Muscular Dystrophy Association, the Joshua Frase Foundation, Cure CMD, Where There's a Will, There's a Cure Foundation, A Foundation Building Strength, the Peter Khuri Myopathy Research Foundation, and sponsored research agreements with Audentes Therapeutics.

Disclosures: Dr Lawlor is a member of the neuromuscular advisory board for Audentes Therapeutics, and has been supported by sponsored research agreements by Audentes Therapeutics. He is also a paid consultant for Sarepta Therapeutics and a scientific collaborator with Acceleron Pharma and Pfizer. Dr Beggs is an inventor of a patent for gene therapy in X-linked myotubular myopathy and a member of the scientific advisory Board of Audentes Therapeutics. Dr Buj-Bello is an inventor of a patent for gene therapy in X-linked myotubular myopathy and a scientific advisor for Audentes Therapeutics. Dr Childers is an inventor on a patent for gene therapy in X-linked myotubular myopathy and a member of the scientific advisory Board of Audentes Therapeutics. Drs. James and Prasad are employees and shareholders of Audentes Therapeutics. Dr Moore has fee-for-service consulting agreements with Sarepta Therapeutics, Audentes Therapeutics, and Flagship Biosciences. Dr Schoser is a member of the neuromuscular advisory board for Audentes Therapeutics. Dr Sewry is a member of the neuromuscular advisory board for Audentes Therapeutics. She is also a member of the editorial boards of *Neuromuscular Disorders*, *Muscle and Nerve*, associate editor for *Neuropathology and Applied Neurobiology*, and receives royalties for published books. Dr Dowling and Dr Meng have no relevant disclosures.

Supplementary Data can be found at http://www.jnen.oxfordjournals.org.

## Abstract

X-linked myotubular myopathy (XLMTM) is a devastating, rare, congenital myopathy caused by mutations in the *MTM1* gene, resulting in a lack of or dysfunction of the enzyme myotubularin. This leads to severe perinatal weakness and distinctive muscle pathology. It was originally thought that XLMTM was related to developmental arrest in myotube maturation; however, the generation and characterization of several animal models have significantly improved our understanding of clinical and pathological aspects of this disorder. Myotubularin is now known to participate in numerous cellular processes including endosomal trafficking, excitation-contraction coupling, cytoskeletal organization, neuromuscular junction structure, autophagy, and satellite cell proliferation and survival. The available vertebrate models of XLMTM, which vary in severity from complete absence to reduced functional levels of myotubularin, recapitulate features of the human disease to a variable extent. Understanding how pathological endpoints in animals with XLMTM translate to human patients will be essential to interpret preclinical treatment trials and translate therapies into human clinical studies. This review summarizes the published animal models of XLMTM, including those of zebrafish, mice, and dogs, with a focus on their pathological features as compared to those seen in human XLMTM patients.

**Key Words:** Congenital, Centronuclear, Hypotrophy, Myopathy, Myotubular, Myotubularin, Sarcotubular.

## INTRODUCTION

X-linked myotubular myopathy (XLMTM) is a rare, devastating, congenital myopathy that mainly affects infants and children. XLMTM is caused by mutations in the *MTM1* gene, the result of which is a loss of function of the myotubularin protein that leads to severe perinatal weakness and distinctive muscle pathology. While "myotubular myopathy" was first thought to be related to a developmental arrest of myotube maturation (1, 2), the generation and characterization of several animal models over the past 15 years have led to significant advances in our understanding of this disorder. Myotubularin is known to participate in numerous cellular processes including endosomal trafficking, excitation-contraction coupling (ECC), cytoskeletal

organization, neuromuscular junction structure, autophagy, and satellite cell proliferation and survival (3–7). Muscle-specific knockdown of myotubularin in adult mice elicits similar phenotypes, which indicates that myotubularin is essential for these processes throughout life (8). The available vertebrate models of XLMTM recapitulate features of the human disease to a variable extent. Understanding how pathological endpoints in myotubularin-deficient animals translate to human XLMTM patients will be essential for interpretation of preclinical studies of potential treatments and bridging therapies to the human clinical trial stage. This review provides a summary of the published animal models of myotubularin deficiency with a focus on comparing the pathological features of these models with those seen in human XLMTM patients. These pathological abnormalities are summarized in the Table.

## KNOWN FUNCTIONS OF MYOTUBULARIN

Myotubularin belongs to a family of 15 active and inactive phosphatases that act on phosphoinositides, which are lipid messengers that play important roles in membrane identity and protein recruitment (9, 10). Through a common tyrosine phosphatase-like domain, active myotubularin family members dephosphorylate phosphatidylinositol 3-phosphate and phosphatidylinositol 3,5-bisphosphate, key regulators of membrane trafficking and endocytosis (10, 11). The specificity of the different myotubularins for particular organelles, suborganelle domains, and particular membranes is a function of the unique combination of several shared domain structures that target the enzyme to particular phosphatidylinositol pools (9, 11, 12). In animal models, myotubularin appears to localize specifically to the sarcolemma (plasma membrane) and sarcotubular membranes, and regulates a range of functions within skeletal muscle cells (13, 14). The characterization of myotubularin localization in humans is not well studied due to the current lack of robust antibody-based tools. In cardiomyocytes, myotubularin has no reported function, nor any clinical association with cardiac disease, despite its ubiquitous distribution (15). In skeletal muscle, myotubularin is involved in the formation and maintenance of the "triad," the set of juxtaposed sarcoplasmic reticulum (SR) and T-tubule structures responsible for mediating ECC (4, 5, 16, 17). The severely disrupted architecture of the sarcotubular structures in XLMTM patients and myotubularin-deficient animal models leads to abnormal $Ca^{2+}$ exchange at the sarcotubular junction and impaired ECC. Studies of contractile function (4, 18) and myostatin inhibition therapy (19) in myotubularin-deficient mice suggest that this impairment of ECC is a major cause of weakness in XLMTM. Myotubularin also binds to desmin and appears to control assembly of desmin intermediate filaments (6); this interaction may contribute to the organelle mislocalization observed in myotubularin-deficient muscle fibers. Additionally, myotubularin deficiency produces abnormalities of the neuromuscular junction (3) and satellite cell numbers (8, 20, 21), which, in mouse models, likely contributes to progressive disease pathology and contractile dysfunction. Abnormalities in the apoptotic, AKT/mTOR and ubiquitin-proteasome pathways (8, 22, 23), have also been reported in multiple models of myotubularin deficiency; these may further exacerbate the disease pathology and progression.

## PATHOLOGICAL FINDINGS IN HUMAN XLMTM

The diagnosis of XLMTM is often strongly suggested by the histopathology observed in a muscle biopsy. The characteristic light microscopic changes of XLMTM in humans often include: (1) myofiber hypotrophy (smallness), particularly of type 1 fibers, (2) a variable number of large-appearing, central myofiber nuclei spaced at regular intervals along the longitudinal axis, (3) central aggregations of organelles including mitochondria, lysosomes, and SR, (4) pale peripheral halos seen with staining for oxidative enzymes (Fig. 1), and (5) perinuclear vacuole-like areas (24). The central nuclei occur in both fiber types, and their frequencies range from as low as 5% (25) to greater than 50% (26). Central nuclei are often more common in myofibers expressing slow myosin and they can occur in fibers without developmental or fetal myosin, indicating

**TABLE.** Comparison of Pathological Abnormalities in Various Myotubularin-Deficient Vertebrate Models and the Human Disease

| Species | Model | Disability | Nuclear Placement | Organelle Localization | Neuromuscular Junctions | Necklace Fibers |
|---|---|---|---|---|---|---|
| Human | N/A | Severe | Central | Central aggregates with peripheral halos | Abnormal | Present, especially in mild cases or carriers |
| Zebrafish | Morpholino knockdown | Severe | Central | Central aggregates | Abnormal | Not assessed |
| Mouse | *Mtm1* KO | Severe | Internal | Subsarcolemmal aggregates | Abnormal | None |
| | *Mtm1* p.R69C | Moderate | Internal | Subsarcolemmal aggregates | Abnormal | None |
| | $Mtm1^{gt/y}$ | Mild | Internal | Peripheral aggregates | Not assessed | Not assessed |
| Canine | Labrador XLMTM | Moderate to severe | Internal | Peripheral and central aggregates, sometimes with halos | Not assessed | Frequent |

KO, knockout; N/A not applicable; XLMTM, X-linked myotubular myopathy.
Note that fiber size is consistently small and sarcotubular disorganization is consistently disorganized in all models of myotubularin deficiency that have been evaluated for these features.

that they have matured at least in terms of myosin expression. All of these features are often seen in human XLMTM patient muscle at birth (26). Satellite cell numbers may be decreased in human XLMTM biopsies that have been taken as early as 30 weeks of gestational age (26); however, quantitation of satellite cells in human muscle can be difficult because factors such as muscle sampled and fiber typing have to be taken into account (26). Necrosis, peri- and endomysial fibrosis, and inflammation are not features of XLMTM in any species. Ultrastructurally, there is disorganization of the sarcotubular system that produces a dramatic decrease in the number and mislocalization of triads (Fig. 2) (5). Collections of dark tubules, probably of SR origin, can occur (Fig. 2); and other features can include marked absence or disruption of myofibrils and cytoplasmic bodies. Of note, the histopathologic features of XLMTM do not appear to predict clinical severity. Specifically, no relationship has been found between the number of centrally nucleated fibers and clinical outcomes. It has been reported that poorer outcomes have been observed in patients with smaller myofiber size at biopsy (25). Anecdotally, some XLMTM patients with comparatively mild phenotypes show organelle mislocalization in only a small proportion of fibers (Supplementary Data 1). Longitudinal studies of pathological progression in the same human patients have only rarely been reported (27, 28), and a comparison of biopsy and autopsy specimens during our review identified more uniform myofiber smallness in autopsy specimens from XLMTM patients in comparison to the fiber size variation (including numerous hypotrophic fibers) that is typically seen on diagnostic biopsies.

Genetic confirmation of a mutation in the *MTM1* gene is essential for the definitive diagnosis of XLMTM. While the findings described here at the light and electron microscopic level strongly suggest XLMTM, some of these findings may be seen in other severe forms of centronuclear myopathy (CNM) and in congenital myotonic dystrophy (CDM) (24, 29, 30). Cases of CNM with severe clinical presentations due to mutations in *DMN2*, *BIN1*, and *RYR1* may show pathological findings similar to those in XLMTM, including small myofiber size, central nucleation, and central aggregates of organelles with peripheral halos. These pathological features are more commonly associated with mutations in *MTM1*, however, than mutations in *DMN2*, *BIN1*, and *RYR1*. With respect to CDM, the pathological features encountered depend on the patients age and tend to be more severe in early cases. In neonatal cases, myofibers are small, nuclei are central, and oxidative enzyme staining may reveal fibers with a pale peripheral halo and dark central aggregates of organelles. Slow fibers are less frequent in congenital CDM biopsies, in comparison to early XLMTM biopsies (31). No ring fibers or sarcoplasmic masses (areas of abundant acid-phosphatase positive material) are obvious at birth, but these may appear by 12 months of age and these features are not seen in XLMTM. Internal nuclei are increased and prominent, often occurring in long chains. Electron microscopy of CDM biopsies taken in the first year of life show a peripheral zone containing glycogen and myofilaments but lacking organized myofibrils and mitochondria, which contrasts with the central organelle aggregation and loss of sarcotubular organization that is seen in XLMTM.

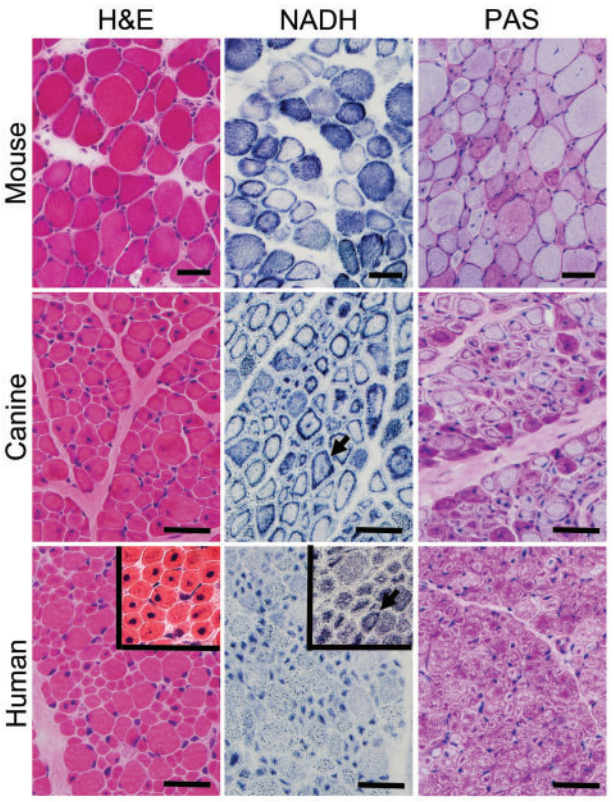


**FIGURE 1.** Pathological findings in murine, canine, and human X-linked myotubular myopathy (XLMTM) by brightfield microscopy. Skeletal muscle from an *Mtm1* knockout mouse at 43 days of life (mid-stage) are shown in comparison to an autopsy specimen from an 18-week-old (end-stage) canine with XLMTM and a diagnostic biopsy of a 2-month-old boy with XLMTM. Hematoxylin and eosin (H&E) staining reveals abnormal fiber size variation and the extent of central or internal nucleation in each affected species. In addition to the hypotrophy of some fibers seen at all disease stages, XLMTM shows marked atrophy of essentially all fibers in the terminal stage; therefore, the apparent difference in myofiber size between the murine (mid-stage) and canine models (end-stage) shown likely relates to disease stage. The percentage of centrally nucleated fibers can vary markedly among patients (H&E inset). Stains for reduced nicotinamide adenine dinucleotide (NADH, also known as NADH-TR) and periodic acid-Schiff (PAS) stain illustrate the patterns of organelle (mitochondrial/sarcotubular) and glycogen mislocalization, respectively, with pale peripheral halos in the human case but dark peripheral staining in the dog and mouse. Mouse tissue typically shows subsarcolemmal aggregation of mitochondria whereas true "necklace fibers" (arrows) can be seen in canine and some human (NADH inset) patient biopsies, as well as in rare fibers in the mouse. Scale bar = 40 μm.

Antibodies against muscleblind-like 1 (MNBL1) are helpful for distinguishing CDM cases from CNMs, including myotubular myopathy, as the latter are negative, while CDM biopsies show anti-MBNL1 positively stained nuclear foci (32–34).

Most women carrying mutations in *MTM1* (XLMTM carriers) are asymptomatic (35). There are reports, however, of

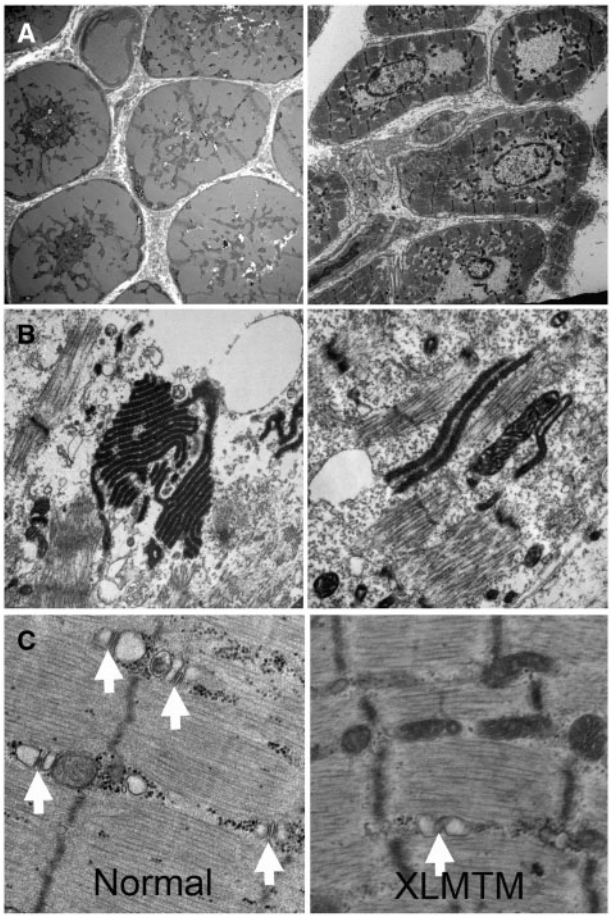


**FIGURE 2.** Ultrastructural findings in human X-linked myotubular myopathy (XLMTM). **(A)** Low-power ultrastructural evaluations of XLMTM muscle reveal centrally located nuclei and central aggregates of organelles including mitochondria (left) and areas with only nuclei and glycogen (right). **(B, C)** Higher power shows organizational abnormalities of the sarcotubular system. Stacks of tubules (probably originating from triads) can be seen in a variety of configurations in the intermyofibrillar space, some of which contain osmiophilic material **(B)**. There is also a lack of well-defined triad structures (white arrows) in XLMTM muscle in contrast to what is seen in normal muscle **(C)**.

XLMTM carriers with myopathic symptoms and pathology consistent with CNM. The clinical severity of these symptomatic XLMTM carriers ranges broadly from severe neonatal weakness (extremely rare) to mild/moderate weakness with a normal lifespan. This broad range of symptomatic severities probably reflects skewed inactivation of the X chromosome (lyonization), where symptomatic XLMTM carriers have more lyonization of the normal *MTM1* allele than those carriers with no symptoms (35–38). The pathology in the reported cases is variable (Supplementary Data 1), but (in contrast to XLMTM male patients) the degree of XLMTM pathology does tend to correlate with the level of clinical severity. Biopsy findings in XLMTM carriers with symptoms during infancy were very similar to those seen in male patients, including myofiber smallness, numerous centrally nucleated fibers, type 1 fiber predominance, central aggregations of organelles, and peripheral halos (36, 39). In addition, necklace fibers with a basophilic loop a few microns beneath the sarcolemma, and associated with internal nuclei, can be a feature of female carriers and milder cases, but may be less common in severe cases (40). XLMTM carriers identified during adulthood display slightly different muscle pathology to those identified in infancy. While carriers with infantile onset tend to have severe disease and pathology similar to affected XLMTM boys, those with later onset display pathological findings including increased fiber size variation (due to the presence of large and small fibers), numerous fibers containing internal nuclei (with a subpopulation of centrally nucleated fibers), and occasional perinuclear vacuole-like areas (37, 38). As such, the pathology of these adult symptomatic XLMTM carriers is more similar to non-XLMTM cases of CNM; this should be a diagnostic consideration when encountering CNM in adult female patients.

## ZEBRAFISH MODEL OF XLMTM

The zebrafish knockdown model of myotubularin deficiency was created using antisense morpholinos to generate embryos with reduced myotubularin protein expression (5). Similar to human XLMTM patients, the zebrafish knockdown model exhibits severe impairment of motor function, muscle fiber hypotrophy, and large-appearing, abnormally located nuclei (Fig. 3). Phenotypic effects are evident very early in the development process. By 24 hours postfertilization, embryos have abnormal dorsal curvature through the back and tail and significantly fewer spontaneous muscle contractions. By 72 hours postfertilization, embryos typically have thinning of the muscle compartment and bent and/or foreshortened tails that correlate with markedly decreased ability to hatch from their chorions, poor touch-evoked escape responses, and diminished swimming capacity.

Pathologically, the zebrafish knockdown model displays findings similar to those seen in human XLMTM patients, including myofiber smallness, centrally nucleated fibers, and mislocalization of organelles (5). There is also ultrastructural disarray of the sarcotubular system that is similar to that seen in human myotubularin deficiency (Fig. 3) (5). The neuromuscular junction in myotubularin-deficient zebrafish, as observed using α-bungarotoxin staining, shows normal-appearing neuronal input but abnormal organization, which is reflected as sparse staining that is generally located in the middle of the myofiber (41). Treatment with an acetylcholinesterase inhibitor strongly improved deficits in spontaneous coiling and touch-evoked escape behaviors, supporting the association between myotubularin support of membrane trafficking and regulation of acetylcholine receptors (42, 43). A similar, albeit less dramatic, response to acetyl cholinesterase inhibitors has also been observed in human cases of XLMTM (41).

Ultrastructural analysis of morpholino-treated zebrafish muscle tissue shows grossly aberrant SR and T-tubule networks (5). SR networks are irregular, disorganized, and often randomly interspersed throughout the sarcomere. Abnormalities in T-tubule structures range from mild changes in triad electron density to fibers with nearly unrecognizable SR/triad regions. These

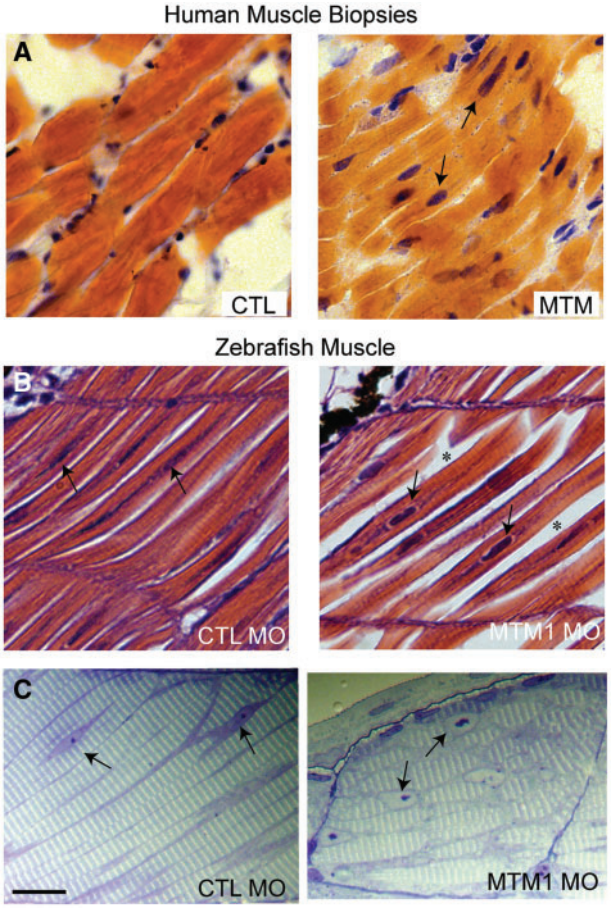


**FIGURE 3.** Pathological findings in human and zebrafish X-linked myotubular myopathy (XLMTM). **(A)** Hematoxylin and eosin (H&E)-stained longitudinal myofibers from myotubular myopathy (MTM) and age-matched control (CTL) human muscle biopsies. Arrows indicate abnormal nuclei. **(B)** H&E-stained longitudinal myofibers from zebrafish control (CTL MO) and myotubularin morphant (MTM MO) 72-hour-post-fertilization embryos. Myonuclei are abnormally rounded (arrows), and there is increased space between fibers in the morphant (*). **(C)** Toluidine blue-stained semi-thin sections from 72-hour-postfertilization morphants. Myonuclei from myotubularin morphants are large, abnormally rounded, and contain discrete nucleoli (arrows). Sarcomeric units are normal in appearance. Scale bar = 20 μm. Reproduced with permission from Dowling JJ, Vreede AP, Low SE et al. Loss of myotubularin function results in T-tubule disorganization in zebrafish and human myotubular myopathy. PLoS Genet 2009;5:e100372. Copyright © 2009 Dowling et al.

alterations in the T-tubule and SR networks, which resemble human pathology, are related to functional impairments in ECC.

## MOUSE MODELS OF XLMTM

The first animal model of XLMTM, the *Mtm1* knockout (KO) mouse (also called the *Mtm1*δ4 mouse), was produced through a large deletion in exon 4 of *Mtm1*(44). *Mtm1* KO mice show weakness starting at approximately 3 weeks of life that progresses to death in a fairly uniform timescale (usually around 5–7 weeks of life, range 4–14 weeks, depending on the background strain) (19, 44). Abnormal nuclear placement is observed in *Mtm1* KO muscle at a lower percentage of muscle fibers than is usually observed in human XLMTM patients, and the placement of these nuclei is typically eccentric rather than central (Fig. 1). A similar "internally nucleated fiber" phenotype is observed in other murine and canine models of myotubularin deficiency. The number of internally nucleated fibers is essentially normal during the perinatal period in *Mtm1* KO mice and this gradually increases with age to between 5% and 45% of fibers at end-stage disease. *Mtm1* KO mice show marked myofiber hypotrophy in at least a subset of fibers (including both oxidative and glycolytic fibers), and this is most apparent after 3 weeks of age when fibers are mature. At this stage of disease, fiber smallness is most consistent with a hypotrophic process rather than an atrophic process, based on fiber shape at the light microscopic level and the absence of redundant basal lamina at the ultrastructural level. Organelle mislocalization occurs in myofibers of *Mtm1* KO mice, with fibers that contain perinuclear central accumulation of mitochondria, but the pattern is most frequently that of a peripheral ring of mitochondria at the sarcolemma and markedly decreased numbers of mitochondria in the central areas of the fiber (and thus somewhat distinct from the patterns seen in canines and humans) (Fig. 1) (4, 19, 44). Sarcotubular elements are also aggregated in the same locations as the mitochondria, which can be clearly visualized on immunostaining for the ryanodine receptor (RYR1) and the dihydropyridine receptor α (DHPR-α) (Fig. 4) (4). By electron microscopy, there is disorganization of the sarcotubular system, with presence of longitudinal tubules (L-tubules) and a decrease in triad number similar to that seen in human XLMTM (4, 5, 18). Organelle mislocalization and triad disorganization are the earliest described pathological signs of the disease in these mice, and progress over time (4).

The availability of the *Mtm1* KO model has allowed systematic evaluations of disease pathology in the context of disease progression and the spectrum of disease severity among several different muscles. Progression of disease in *Mtm1* KO mice generally correlates with increasing numbers of myofibers displaying characteristic XLMTM-like pathology: myofiber smallness and organelle mislocalization. These features are found in nearly all fibers by the time the mice are killed due to symptomatic severity between 4 and 14 weeks of life (19, 44). Myofiber smallness at late stages of disease is probably caused by a combination of hypotrophy and atrophy, as average fiber size decreases during terminal phases of disease. As noted above, the number of fibers with internal nuclei also increases with age. Approximately 5% to 45% of fibers have internal nuclei in most *Mtm1* KO mice by the end of the disease course, but this percentage varies depending on the muscle in the body and strain background (4, 13). The number of muscle satellite cells in *Mtm1* KO mice decreases with age to approximately 30% of wild-type values at late disease stages (20). Neuromuscular junctions are enlarged and less complex than normal at the ultrastructural level (3). Whole-muscle ex vivo contractile function in extensor digitorum longus and

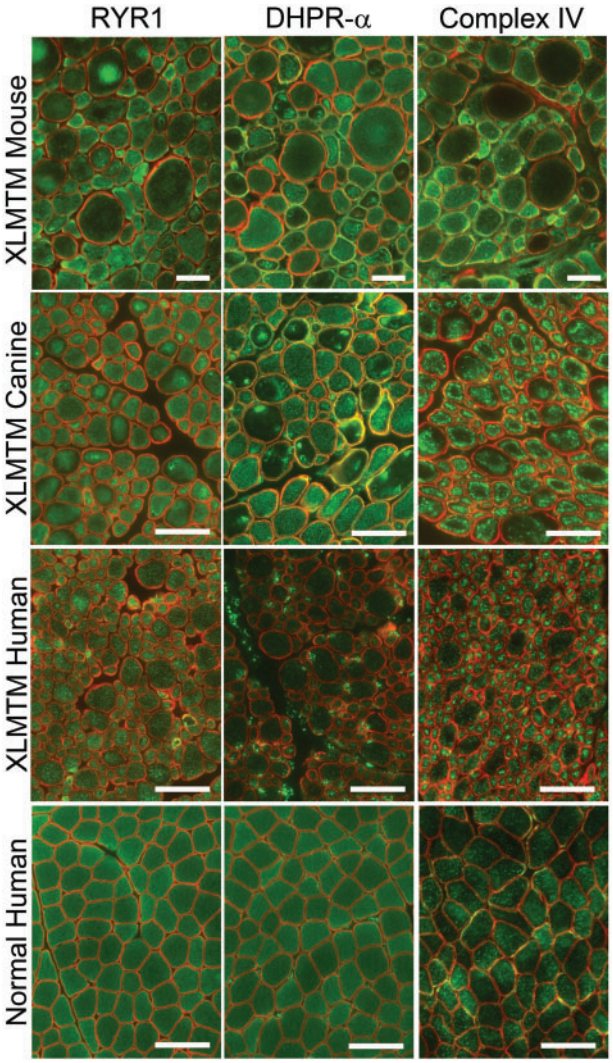


**FIGURE 4.** Immunofluorescence patterns of organelle mislocalization in X-linked myotubular myopathy (XLMTM). Abnormalities of organelle localization are seen to varying degrees in the mouse and dog models using antibodies against the ryanodine receptor (RYR1) and the dihydropyridine receptor α (DHPR-α), which are found on the sarcoplasmic reticulum and T-tubules, respectively. Staining for RYR1 displays varying degrees of abnormal organelle aggregation in each model, although this is more difficult to appreciate in comparison to reduced nicotinamide adenine dinucleotide (NADH-TR) staining. Staining for DHPR-α shows a similar pattern of mislocalization in murine and canine XLMTM, but organelle mislocalization cannot be clearly visualized on human XLMTM tissue. Immunostaining for electron transport chain complex IV shows clear mitochondrial mislocalization in mouse, canine, and human XLMTM. Staining of human muscle biopsy tissue without pathological findings ("Normal Human") displays even intracellular staining for all 3 antigens. Staining for RYR1, DHPR-α, and cytochrome oxidase (COX) are shown on the green channel, with dystrophin immunostaining shown on the red channel to highlight myofiber edges. Scale bar = 50 μm.

soleus muscles of *Mtm1* KO mice showed impaired contractile force, with slightly better performance seen in the predominantly oxidative soleus muscle than in the predominantly glycolytic extensor digitorum longus muscle (18). In contrast, skinned fiber preparations using *Mtm1* KO myofibers showed equivalent function between slow and fast myofibers, suggesting that the better performance in oxidative muscles noted above was due to a factor (perhaps mitochondria) that was removed or destroyed during the chemical skinning process.

*Mtm1* KO mice are the most frequently used model for preclinical treatment trials, and a variety of pathological recovery patterns have been seen. An early study using intramuscular injection of adeno-associated virus (AAV) carrying the *Mtm1* coding sequence (AAV8-Mtm1) showed complete correction of XLMTM pathology at the light microscopic level in the injected limbs (13). Correction of pathology was seen across all muscle groups, and the lifespan of the mice was extended beyond 6 months after a single dose of the vector at 9 weeks of age (45). Concurrently, a targeted enzyme replacement agent (3E10Fv-MTM1) was developed that combined enzymatically active myotubularin with an antibody fragment that improved distribution to muscle. Proof-of-concept pilot studies using local injections of a nonoptimized 3E10Fv-MTM1 dose over 2 weeks showed improvements in single-muscle strength and sarcotubular ultrastructural organization, whereas XLMTM pathology at the light microscopic level was unchanged (18). In contrast, a trial of the myostatin inhibitor, ActRIIB-mFc, produced dramatic improvement of glycolytic fiber size but with minimal benefits to lifespan or strength (19). Because ActRIIB-mFc provided a means of mitigating myofiber hypotrophy without affecting the other pathological features of myotubularin deficiency, these studies suggest that abnormalities of organelle localization and/or ECC comprise the predominant cause(s) of weakness in these mice. This concept is further supported by the comparison of functional studies using whole-muscle versus skinned fiber preparations, which reveal a large component of contractile deficit that is only apparent when membranous structures are intact (18). While this component of weakness may be due to abnormalities in the sarcolemma, mitochondria, or sarcotubular system, the known abnormalities of sarcotubular organization and calcium handling suggest that ECC impairment is a major factor.

## TISSUE-SPECIFIC *MTM1* KO MICE

There have been several studies to induce myotubularin deficiency to specific tissues and/or time periods. Conditional *Mtm1* KO mice that were myotubularin deficient only in skeletal muscle (using a transgenic line that expresses Cre recombinase under the skeletal muscle α-actin promoter) showed a phenotype that was indistinguishable from *Mtm1* KO mice (44). In contrast, conditional *Mtm1* KO mice that were myotubularin deficient in the central nervous system but not skeletal muscle (using a transgenic line expressing Cre recombinase under the neuron-specific enolase promoter) did not show any obvious clinical or pathological phenotype. To study the impact of myotubularin deficiency on adult muscle, a recombinant AAV that expresses Cre recombinase under the muscle-

specific desmin promoter was injected locally into the muscle of adult conditional *Mtm1* KO mice (8). Myotubularin deficiency in these muscles produced weakness and pathology that was strikingly similar to the effects of germline mutations in *Mtm1*, including progressive decreases in myofiber size, mislocalization of organelles, increases in the number of internally nucleated fibers, and abnormal sarcotubular morphology on electron microscopy. The number of satellite cells progressively decreased in myotubularin-deficient adult muscles, and abnormalities in proteins related to Akt signaling, neuromuscular transmission, and autophagy were also observed.

## *MTM1* p.R69C MICE

The *Mtm1* p.R69C mouse was designed to produce a less severe myotubularin deficiency phenotype by "knocking in" the c.205C>T mutation that had been found in several human XLMTM patients who survived past infancy (46). As predicted, *Mtm1* p.R69C mice have greater strength than *Mtm1* KO mice, and lifespans often exceeding 1 year. Similar to the pathology seen in *Mtm1* KO mice, affected myofibers display hypotrophy and mislocalization of organelles (as described above). As observed in the *Mtm1* KO and canine XLMTM models, there is abnormal localization of nuclei, which are usually eccentric rather than central. This pattern is slightly different from that seen in human XLMTM, where nuclear placement tends to be central rather than eccentric. The number of internally nucleated fibers may only be mildly increased (21, 46). Neuromuscular junctions are enlarged and have less complex junctional folds than are seen in wild-type mice (3). Satellite cell depletion is noted at late stages of disease in these mice (21). It should be noted that the *Mtm1* p.R69C mutation functions as a splice site mutation leading to the expression of only a very small amount of full-length mutant myotubularin transcript, and a similar impact on splicing has been observed in human tissue harboring the *MTM1* p.R69C mutation (46). This suggests that induction of very small amounts of myotubularin may produce substantial clinical benefits in the myotubularin-null state.

*Mtm1* p.R69C mice have been used in several published trials of potential treatments for XLMTM. Pyridostigmine (an acetylcholinesterase inhibitor that improves neuromuscular transmission) produced improvements in grip strength and endurance (3) as has been found in some human cases (41), but evaluations of treatment effects on histopathology were not performed. Localized wild-type myoblast transplantation into the gastrocnemius muscle of *Mtm1* p.R69C mice produced increases in muscle mass and evoked muscle action potentials, but increases in fiber size were not observed and other pathological features were not assessed (47). Additionally, a study of myostatin inhibition using ActRIIB-mFc in *Mtm1* p.R69C mice identified some muscle-specific phenotypes in these mice. Treated mice developed hypertrophy of glycolytic myofibers only in the gastrocnemius muscle, without apparent effect in other muscles such as the quadriceps or triceps (21). This was markedly different from the effects observed in the *Mtm1* KO model using the same agent, which produced significant hypertrophy in all of these major muscles (19). Subsequent studies identified differences between the *Mtm1* p.R69C quadriceps and gastrocnemius muscles with respect to satellite cell behavior and hypertrophic signaling that may have been associated with differential treatment responses in these animals (21). While the precise mechanism(s) responsible for these different responses remains unclear, the results established that treatment studies using the mouse models should be cautiously designed, and analysis of various muscle groups is advisable.

## *MTM1*$^{gt/y}$ MICE

An *Mtm1* mutant mouse with a truncating mutation in exon 1 of *Mtm1* has been described in a single publication (23). The *Mtm1*$^{gt/y}$ mice are similar in weight to wild-type animals until approximately 4 weeks of age, and, therefore, have a less severe phenotype than *Mtm1* KO mice. Muscle pathology in *Mtm1*$^{gt/y}$ appears similar to other myotubularin-deficient mice, including myofiber smallness, subsarcolemmal organelle localization, mild increases in the number of internal nuclei, and ultrastructural sarcotubular disorganization. A blockage of a late stage of autophagy was detected in these mice, resulting in protein aggregates that are positive for ubiquitin and p62. Such protein inclusions have not been reported in other models of XLMTM, although other studies in *Mtm1* KO mice showed dysregulation of autophagy and ubiquitin-proteasome pathways that resulted in ultrastructurally abnormal autophagosomes (8, 22). Analysis of *Mtm1*$^{gt/y}$ mice also revealed abnormalities of mitochondrial structure including mitochondria with fewer decondensed and swollen cristae (23), which can be seen to some extent across all XLMTM models studied. The degree to which mitochondrial structural abnormalities are due to primary mitochondrial dysfunction versus secondary effects is currently unclear.

## CANINE XLMTM

X-linked myotubular myopathy in dogs was discovered as a naturally occurring disease in several related litters of Labrador Retriever (*MTM1* p.N155K) puppies (14). This led to the establishment of a XLMTM canine colony that has been instrumental for preclinical studies in this canine model. XLMTM Labradors, and subsequent generations bred onto a beagle background, appear phenotypically normal at birth, but by 8 weeks of age, they begin to display a characteristic "slack jaw" appearance. Shortly thereafter, XLMTM puppies display subtle hind limb muscle weakness, gait abnormalities, and reduced physical activity. Ultimately, these clinical impairments progress until death becomes necessary between 15 and 26 weeks of age (14). Affected dogs exhibit muscle pathology similar to the *Mtm1* KO and *Mtm1* p.R69C murine models, including myofiber hypotrophy (of both slow and fast fibers), mild-to-moderate increases in the number of internally nucleated fibers, mislocalization of organelles, and disorganization of the sarcotubular system at the ultrastructural level (14, 45). All of these features are present in a subpopulation of fibers at 10 weeks of life, and they tend to affect greater numbers of fibers as the disease progresses. One remarkable pathologic feature of canine XLMTM is a pattern of organelle mislocalization distinctively different from both murine and human XLMTM. Whereas the pattern of organelle/mitochondrial

mislocalization in humans tends to be a central aggregation, and in murine models tends to be subsarcolemmal (necklace-like), XLMTM Labradors and "Lab-beagles" show a combination of central organelle aggregation, true necklace fibers, and fibers with necklace-like subsarcolemmal organelle aggregates (14, 45). In cases where these aggregates are associated with internalized nuclei along the same line, they can be considered true "necklace fibers" that have been reported in a range of CNMs. Similar to that demonstrated in *Mtm1* KO mice, these aggregates of mislocalized organelles stain for markers of mitochondria (complex IV), T-tubules (DHPR-α), and SR (RYR1) (Fig. 4) (14). While the varying patterns of organelle mislocalization across different myotubularin-deficient models likely represent different aspects of a similar pathogenic process, it is important to recognize this spectrum of patterns when considering how best to evaluate and quantify pathological features. A pilot study assessing satellite cell number in the vastus lateralis and gastrocnemius muscles of XLMTM Lab-beagles comparing satellite cell numbers at 10 and 17 weeks of age did not show satellite cell depletion (unpublished). It should also be noted that canine XLMTM carriers do not show weakness or any sign of MTM pathology in any of the studies performed thus far, despite extensive evaluation. Canine XLMTM has also recently been reported in Rottweiler dogs (*MTM1* p.Q384P) (48), which showed extensive similarities to the *MTM1* p.N155K dogs, both in terms of pathological findings and clinical features.

The canine *MTM1* p.N155K XLMTM model has been used to test gene therapy for XLMTM (AAV8-MTM1—a recombinant AAV8 vector, carrying the canine *MTM1* cDNA under control of the desmin promoter) in a pilot study (45). Intramuscular injections of AAV8-MTM1 in hind limb cranial tibialis muscles demonstrated dramatic and rapid improvements in strength and a concomitant reversal of XLMTM pathology (including resolution of myofiber hypotrophy, organelle mislocalization, number of centrally nucleated fibers, and sarcotubular organization) in the injected limb in comparison with contralateral saline-injected limbs (45). Follow-up studies using systemic AAV8-MTM1 administered intravenously produced similar histopathologic and functional improvements in all muscles sampled for at least 1 year after a single dose (45), and further systemic dosing and long-term follow-on studies are in progress. Based on these encouraging results, clinical studies utilizing gene therapy are now planned.

## CONCLUSION

XLMTM is a severe congenital myopathy with characteristic pathological findings in most cases, including myofiber hypotrophy, centrally nucleated myofibers, and mislocalization of organelles. When comparing myotubularin-deficient fish, mice, and dogs to human patients, there are many similarities in pathology, but there are also some differences in how these abnormalities manifest (Table). Such variation needs to be accounted for when designing strategies for the quantitation of pathological findings in XLMTM, and our group is currently developing techniques that address these issues. As therapeutic development progresses from nonclinical to clinical studies in XLMTM, an understanding of the impact of myotubularin deficiency in each species is essential for the appropriate design of pathological endpoints using human muscle tissue, and indeed for understanding the translatability of findings in an animal model to humans.

## ACKNOWLEDGMENTS

*Some images in this publication were produced with the resources of the Children's Hospital of Wisconsin Research Institute's Imaging Core Facility and the electron microscopy core facility at the Medical College of Wisconsin. We would also like to thank Dr Magda Morton for her editorial assistance.*

## REFERENCES

1. Spiro AJ, Shy GM, Gonatas NK. Myotubular myopathy. Persistence of fetal muscle in an adolescent boy. Arch Neurol 1966;14:1–14
2. van Wijngaarden GK, Fleury P, Bethlem J, et al. Familial "myotubular" myopathy. Neurology 1969;19:901–8
3. Dowling JJ, Joubert R, Low SE, et al. Myotubular myopathy and the neuromuscular junction: A novel therapeutic approach from mouse models. Dis Model Mech 2012;5:852–9
4. Al-Qusairi L, Weiss N, Toussaint A, et al. T-tubule disorganization and defective excitation-contraction coupling in muscle fibers lacking myotubularin lipid phosphatase. Proc Natl Acad Sci U S A 2009;106:18763–8
5. Dowling JJ, Vreede AP, Low SE, et al. Loss of myotubularin function results in T-tubule disorganization in zebrafish and human myotubular myopathy. PLoS Genet 2009;5:e1000372
6. Hnia K, Tronchere H, Tomczak KK, et al. Myotubularin controls desmin intermediate filament architecture and mitochondrial dynamics in human and mouse skeletal muscle. J Clin Invest 2011;121:70–85
7. Tsujita K, Itoh T, Ijuin T, et al. Myotubularin regulates the function of the late endosome through the gram domain-phosphatidylinositol 3,5-bisphosphate interaction. J Biol Chem 2004;279:13817–24
8. Joubert R, Vignaud A, Le M, et al. Site-specific Mtm1 mutagenesis by an AAV-Cre vector reveals that myotubularin is essential in adult muscle. Hum Mol Genet 2013;22:1856–66
9. Vicinanza M, D'Angelo G, Di Campli A, et al. Function and dysfunction of the PI system in membrane trafficking. EMBO J 2008;27:2457–70
10. Cowling BS, Toussaint A, Muller J, et al. Defective membrane remodeling in neuromuscular diseases: Insights from animal models. PLoS Genet 2012;8:e1002595
11. Laporte J, Bedez F, Bolino A, et al. Myotubularins, a large disease-associated family of cooperating catalytically active and inactive phosphoinositides phosphatases. Hum Mol Genet 2003;12 Spec No 2:R285–92
12. Mruk DD, Cheng CY. The myotubularin family of lipid phosphatases in disease and in spermatogenesis. Biochem J 2011;433:253–62
13. Buj-Bello A, Fougerousse F, Schwab Y, et al. AAV-mediated intramuscular delivery of myotubularin corrects the myotubular myopathy phenotype in targeted murine muscle and suggests a function in plasma membrane homeostasis. Hum Mol Genet 2008;17:2132–43
14. Beggs AH, Bohm J, Snead E, et al. MTM1 mutation associated with X-linked myotubular myopathy in Labrador Retrievers. Proc Natl Acad Sci U S A 2010;107:14697–702
15. Das S, Dowling J, Pierson CR. X-linked centronuclear myopathy. NCBI Bookshelf, GeneReviews 2002.
16. Al-Qusairi L, Laporte J. T-tubule biogenesis and triad formation in skeletal muscle and implication in human diseases. Skelet Muscle 2011;1:26
17. Cowling BS, Chevremont T, Prokic I, et al. Reducing dynamin 2 expression rescues X-linked centronuclear myopathy. J Clin Invest 2014;124:1350–63
18. Lawlor MW, Armstrong D, Viola MG, et al. Enzyme replacement therapy rescues weakness and improves muscle pathology in mice with X-linked myotubular myopathy. Hum Mol Genet 2013;22:1525–38
19. Lawlor MW, Read BP, Edelstein R, et al. Inhibition of activin receptor type IIb increases strength and lifespan in myotubularin-deficient mice. Am J Pathol 2011;178:784–93
20. Lawlor MW, Alexander MS, Viola MG, et al. Myotubularin-deficient myoblasts display increased apoptosis, delayed proliferation, and poor cell engraftment. Am J Pathol 2012;181:961–8

21. Lawlor MW, Viola MG, Meng H, et al. Differential muscle hypertrophy is associated with satellite cell numbers and Akt pathway activation following activin Type IIB receptor inhibition in Mtm1 p.R69C mice. Am J Pathol 2014;184:1831–42
22. Al-Qusairi L, Prokic I, Amoasii L, et al. Lack of myotubularin (MTM1) leads to muscle hypotrophy through unbalanced regulation of the autophagy and ubiquitin-proteasome pathways. FASEB J 2013;27:3384–94
23. Fetalvero KM, Yu Y, Goetschkes M, et al. Defective autophagy and mTORC1 signaling in myotubularin null mice. Mol Cell Biol 2013;33:98–110
24. Dubowitz V, Sewry C, Oldfors A. Congenital myopathies and related disorders. In: *Muscle Biopsy: A Practical Approach 4th Edn*. Oxford: Elsevier 2013:358–405
25. Pierson CR, Agrawal PB, Blasko J, et al. Myofiber size correlates with MTM1 mutation type and outcome in X-linked myotubular myopathy. Neuromuscul Disord 2007;17:562–8
26. Shichiji M, Biancalana V, Fardeau M, et al. Extensive morphological and immunohistochemical characterization in myotubular myopathy. Brain Behav 2013;3:476–86
27. de Goede CG, Kelsey A, Kingston H, et al. Muscle biopsy without centrally located nuclei in a male child with mild X-linked myotubular myopathy. Dev Med Child Neurol 2005;47:835–7
28. Helliwell TR, Ellis IH, Appleton RE. Myotubular myopathy: Morphological, immunohistochemical and clinical variation. Neuromuscul Disord 1998;8:152–61
29. Dubowitz V, Sewry C, Oldfors A. Muscular dystrophies and allied disorders: Facioscapulohumeral, myotonic, and oculopharyngeal muscular dystrophies. In: *Muscle Biopsy: A Practical Approach 4th Edn*. Oxford: Elsevier 2013
30. Jungbluth H, Gautel M. Pathogenic mechanisms in centronuclear myopathies. Front Aging Neurosci 2014;6:339
31. Soussi-Yanicostas N, Chevallay M, Laurent-Winter C, et al. Distinct contractile protein profile in congenital myotonic dystrophy and X-linked myotubular myopathy. Neuromuscul Disord 1991;1:103–11.
32. Schoser B. Muscle diseases with DNA expansions. In: Goebel HH, Sewry C, Weller RO, eds. *Muscle Disease: Pathology and Genetics*. Oxford: Wiley Blackwell 2013:273–83
33. Holt I, Jacquemin V, Fardaei M, et al. Muscleblind-like proteins: Similarities and differences in normal and myotonic dystrophy muscle. Am J Pathol 2009;174:216–27
34. Sewry CA, Quinlivan RC, Squier W, et al. A rapid immunohistochemical test to distinguish congenital myotonic dystrophy from X-linked myotubular myopathy. Neuromuscul Disord 2012;22:225–30
35. Kristiansen M, Knudsen GP, Tanner SM, et al. X-inactivation patterns in carriers of X-linked myotubular myopathy. Neuromuscul Disord 2003;13:468–71
36. Jungbluth H, Sewry CA, Buj-Bello A, et al. Early and severe presentation of X-linked myotubular myopathy in a girl with skewed X-inactivation. Neuromuscul Disord 2003;13:55–9
37. Tanner SM, Orstavik KH, Kristiansen M, et al. Skewed X-inactivation in a manifesting carrier of X-linked myotubular myopathy and in her non-manifesting carrier mother. Human Genet 1999;104:249–53
38. Penisson-Besnier I, Biancalana V, Reynier P, et al. Diagnosis of myotubular myopathy in the oldest known manifesting female carrier: A clinical and genetic study. Neuromuscul Disord 2007;17:180–5
39. Dahl N, Hu LJ, Chery M, et al. Myotubular myopathy in a girl with a deletion at Xq27-q28 and unbalanced X inactivation assigns the MTM1 gene to a 600-kb region. Am J Human Genet 1995;56:1108–15
40. Bevilacqua JA, Bitoun M, Biancalana V, et al. "Necklace" fibers, a new histological marker of late-onset MTM1-related centronuclear myopathy. Acta Neuropathol 2009;117:283–91
41. Robb SA, Sewry CA, Dowling JJ, et al. Impaired neuromuscular transmission and response to acetylcholinesterase inhibitors in centronuclear myopathies. Neuromuscul Disord 2011;21:379–86
42. Kumari S, Borroni V, Chaudhry A, et al. Nicotinic acetylcholine receptor is internalized via a Rac-dependent, dynamin-independent endocytic pathway. J Cell Biol 2008;181:1179–93
43. Nicot AS, Laporte J. Endosomal phosphoinositides and human diseases. Traffic 2008;9:1240–9
44. Buj-Bello A, Laugel V, Messaddeq N, et al. The lipid phosphatase myotubularin is essential for skeletal muscle maintenance but not for myogenesis in mice. Proc Natl Acad Sci U S A 2002;99:15060–5
45. Childers MK, Joubert R, Poulard K, et al. Gene therapy prolongs survival and restores function in murine and canine models of myotubular myopathy. Sci Transl Med 2014;6:220ra10
46. Pierson CR, Dulin-Smith AN, Durban AN, et al. Modeling the human MTM1 p.R69C mutation in murine Mtm1 results in exon 4 skipping and a less severe myotubular myopathy phenotype. Hum Mol Genet 2012;21:811–25
47. Lim HJ, Joo S, Oh SH, et al. Syngeneic myoblast transplantation improves muscle function in a murine model of X-linked myotubular myopathy. Cell Transplant 2015;24:1887–900
48. Shelton GD, Rider BE, Child G, et al. X-linked myotubular myopathy in Rottweiler dogs is caused by a missense mutation in exon 11 of the MTM1 gene. Skelet Muscle 2015;5:1